Multiple "optimum" conditions for Co-Mo catalyzed growth of vertically aligned single-walled carbon nanotube forests

Hisashi Sugime [a], Suguru Noda [a*], Shigeo Maruyama [b], Yukio Yamaguchi [a]

[a] *Department of Chemical System Engineering, School of Engineering, The University of Tokyo, 7-3-1 Hongo, Bunkyo-ku, Tokyo 113-8656, Japan*

[b] *Department of Mechanical Engineering, School of Engineering, The University of Tokyo, 7-3-1 Hongo, Bunkyo-ku, Tokyo 113-8656, Japan*

Abstract

Carbon nanotubes (CNTs) were grown directly on substrates by alcohol catalytic chemical vapor deposition using a Co-Mo binary catalyst. Optimum catalytic and reaction conditions were investigated using a combinatorial catalyst library. High catalytic activity areas on the substrate were identified by mapping the CNT yield against the orthogonal gradient thickness profiles of Co and Mo. The location of these areas shifted with changes in reaction temperature, ethanol pressure and ethanol flow rate. Vertically aligned single-walled CNT (SWCNT) forests grew in several areas to a maximum height of ca. 30 μm in 10 min. A pure Co catalyst yielded a vertically aligned SWCNT forest with a bimodal diameter distribution. The effects of Mo on the formation of catalyst nanoparticles and on the diameter distribution of SWCNTs are discussed and Mo as thin as a monolayer or thinner was found to suppress the

[*] Corresponding author: Tel. +81-3-5841-7330; fax: +81-3-5841-7332. *E-mail Address: noda@chemsys.t.u-tokyo.ac.jp* (S. Noda).

broadening of SWCNT diameter distributions.

1. Introduction

For direct growth of single-walled carbon nanotubes (SWCNTs) on substrates by chemical vapor deposition (CVD) methods, preparation of catalyst nanoparticles is a crucial issue. Many types of metal such as Fe, Co, Ni, Mo, either individually or mixtures of them, have been reported as catalysts, and oxides such as SiO_2, MgO and Al_2O_3 have been used as support materials [1-5]. Vertically aligned SWCNT forests have been grown [6-13]. For example, Co-Mo binary catalysts have effectively been used to grow SWCNT forests on SiO_2 either from carbon monoxide (CO) [4, 5, 11] or from ethanol (C_2H_5OH) [6, 7], although the optimum Co/Mo atomic ratio differed, namely, 1/3 for CO [4, 5, 11], whereas 1.6/1.0 for C_2H_5OH [6, 7]. A phase diagram was used to explain the optimum catalyst conditions for a Fe-Mo system [14, 15]. The structure of catalyst nanoparticles should be affected not only by the composition but also by the amount of catalyst metals. However, although surface atomic concentration of catalyst metals is important, it is difficult to precisely determine this concentration when wet processes such as impregnation or dip coating methods are used for catalyst preparation. Previously, we developed a simple method to prepare a series of catalyst conditions, namely, different composition and amount, on a single substrate by applying a physical mask during catalyst deposition by sputtering [16]. In this study, using this "combinatorial masked deposition" method, or CMD method [17], we systematically investigated carbon nanotube (CNT) growth by alcohol catalytic CVD (ACCVD) [18] with Co-Mo binary catalyst.

2. Experimental

A detailed description of catalyst preparation using the CMD method was

described elsewhere [16]. Briefly, Si substrates (14×14 mm^2) with a 50-nm-thick oxide layer and quartz substrates (14×14 mm^2) were cleaned using a mixture of H_2O_2 (30%) and H_2SO_4 (98%) (1:3) followed by washing with de-ionized water. Mo with a gradient thickness profile was deposited using a conventional RF sputtering system with a physical mask. Then the mask was rotated by 90 °, and Co was deposited on this Mo. In this way, catalyst libraries having orthogonal thickness profiles were obtained. Note that the sequence of Mo and Co deposition had relatively no effect on the CNT yield for regions with Mo/Co thickness around 1 nm or less, where CNTs mainly grew (data not shown).

CNTs were grown in a novel ACCVD apparatus (developed in this study) consisting of a quartz tube (34 mm in inner diameter, 300 mm in length) and electric furnace (Fig. 1). The joints of the four-way flange, the quartz glass tube and the gas lines are located "downstream" from the substrates to ensure negligible leakage contamination. The reactor was heated to and then held at a target CVD temperature (1020, 1120 or 1220 K) for 10 minutes under 5 vol% H_2/Ar flow at 20 sccm and 2.7 kPa to reduce the metals. After this pretreatment, the H_2/Ar flow was then stopped and the reactor was pumped below 50 Pa, and C_2H_5OH was supplied at 1.3, 4.0 or 12 kPa for 10 minutes. The pumping rate was fixed during pretreatment and CVD. C_2H_5OH feed rates were adjusted to realize a target pressure under the fixed pumping rate. At 1120 K, typical C_2H_5OH flow rates were 4.9 sccm for 1.3 kPa, 25 sccm for 4.0 kPa and 140 sccm for 12 kPa. The libraries were characterized by using micro-Raman scattering spectroscopy (Seki Technotron, STR-250 and HORIBA, HR800), optical scanner (EPSON, GT-X700), scanning electron microscopy (SEM, Hitachi, S-900) and transmission electron microscopy (TEM, JEOL, 2000EX).
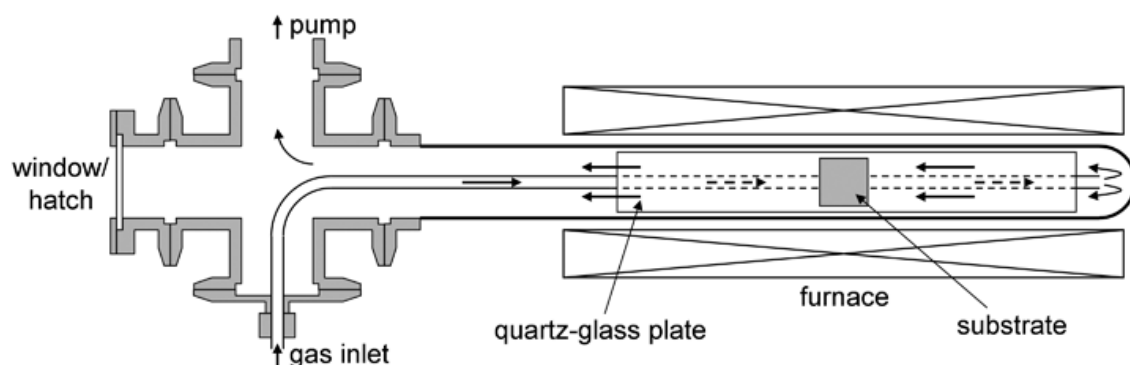
Fig. 1. Top-view schematic of novel ACCVD apparatus

3. Results and Discussion

3.1 *Effect of CVD conditions on areas of high catalytic activity*

Figure 2a shows a schematic of a Co-Mo catalyst library, showing that both Co and Mo had orthogonal gradient thickness profiles. Figure 2b shows the relationship between location on the substrate (i.e., distance from the edge of the substrate) and nominal thickness of Co and Mo. Surface diffusion and aggregation of metals during pretreatment under H_2 atmosphere result in the formation of metallic nanoparticles, some of which have sizes suitable for growing SWCNTs [17]. Size distributions of the nanoparticles were affected by both the composition and amount of Co and Mo. Figure 2c shows photographs of a catalyst library on Si substrates after CVD for different reaction temperature and C_2H_5OH pressure. The black areas roughly correspond to the areas where CNTs grew to a thickness in excess of a few micrometers.

Figure 3 shows Raman spectra taken at 25 different locations (white dots) on a Co/Mo catalyst library in which the samples were excited with an Ar^+-laser irradiation (488.0 nm), the reaction temperature was 1120 K, and C_2H_5OH pressure was 4.0 kPa

(the same sample as shown in the center image in Fig. 2c). At a Mo thickness of 2.2 nm (Fig. 3e), no peaks were observed for carbon products (such as G-band peak at around 1590 cm^{-1} nor D-band peak at around 1350 cm^{-1}). This absence indicates that Co did not catalyze the growth of CNTs on a thick Mo layer and that Mo itself did not have catalytic activity under these conditions (1120 K, and 4.0 kPa) [19]. As the Mo thickness decreased (Figs. 3a-d), G-band appeared. The split shape of G-band and the existence of Radial Breathing Modes (RBMs) at the low-wavenumber region indicate that the products in the black areas contained SWCNTs. The composition and amount of efficient catalyst depended on the CVD conditions such as reaction temperature and C$_2$H$_5$OH pressure (Fig. 2c).
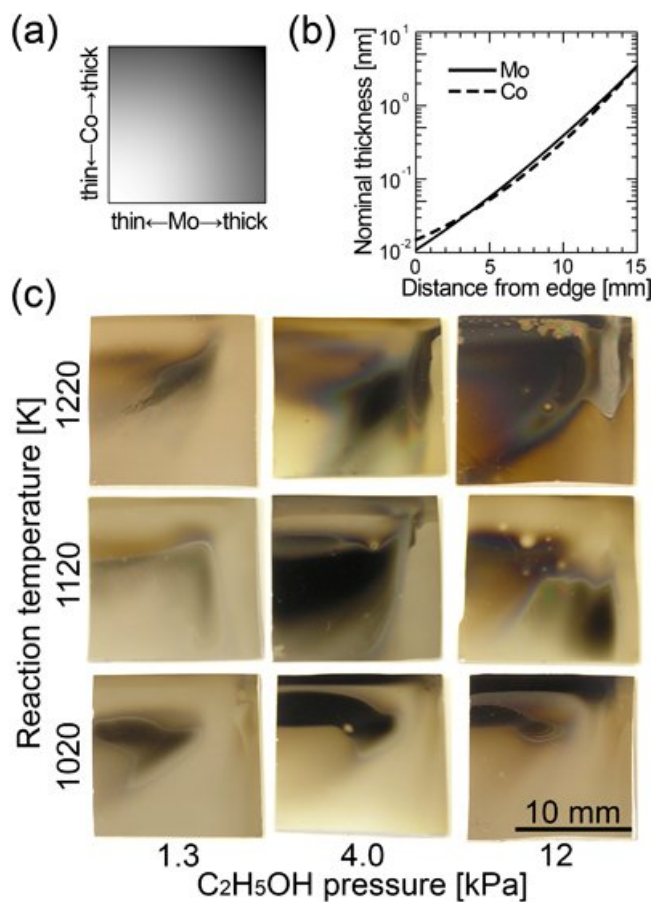
Fig. 2.   Schematic of a Co-Mo catalyst library (a), nominal thickness profiles of Co and Mo within the catalyst library (b), and photographs of the library after ACCVD at different reaction temperature and C_2H_5OH pressure (c).
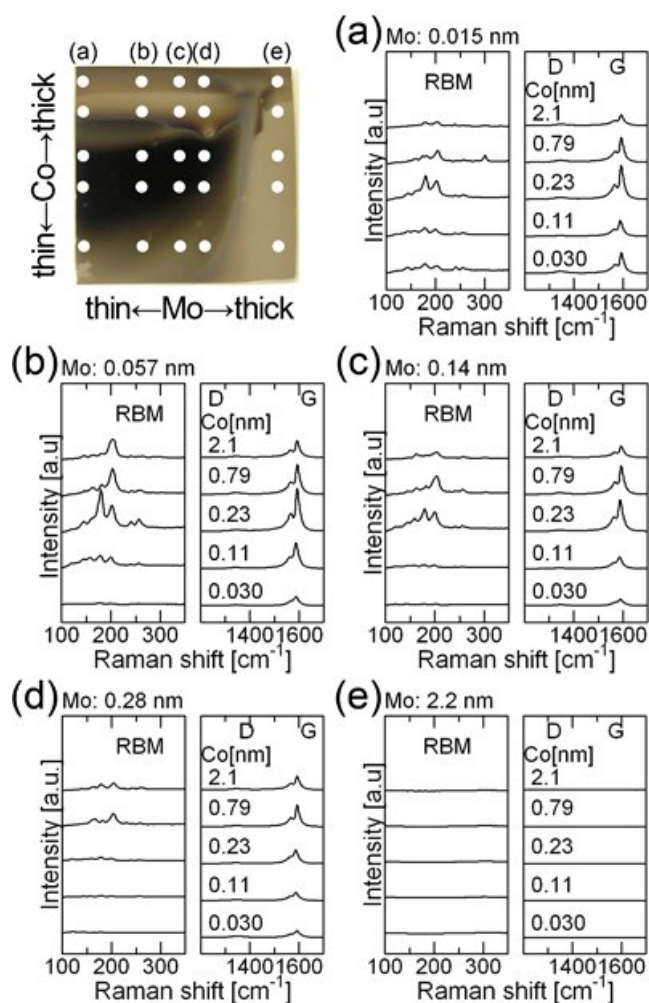

Fig. 3.   Photograph and Raman spectra of a Co-Mo catalyst library after ACCVD at reaction temperature of 1120 K and C_2H_5OH pressure of 4.0 kPa (same sample as that in the center image of Fig. 2c). White dots indicate locations at which Raman spectra were obtained using an Ar^+-laser (488.0 nm) for excitation.

To clarify the areas of catalytic activity, relative CNT yields for catalyst

libraries on quartz glass substrates were estimated qualitatively by using an optical scanner (EPSON, GT-X700) to map the optical transmittance of the CNTs against Co-Mo catalyst conditions. Figure 4 shows maps of the average white light transmittance of the nanotube films on a catalyst library as a function of surface atomic concentrations of Co and Mo for different reaction temperature and C_2H_5OH flow rate (C_2H_5OH pressure was 4.0 kPa for all samples). The diagonal lines in Fig. 4 represent the optimum atomic ratio of Co/Mo previously reported, namely, Co/Mo = 1.6/1.0 [6, 7] for C_2H_5OH feedstock and Co/Mo = 1/3 for CO feedstock [4, 5, 11]. The area where Co/Mo = 1.6/1.0 showed high catalytic activity at the lower reaction temperature of 1120 K (Fig. 4a), whereas at the higher reaction temperature of 1220 K (Fig. 4b), that same area showed reduced catalytic activity and the area where Co/Mo = 1/3 showed enhanced catalytic activity. A similar tendency was observed for a reaction temperature of 1120 K and a lower flow rate of 8.5 sccm (Fig. 4c), namely, catalytic activity was reduced in the area where Co/Mo = 1.6/1.0 but enhanced in the area where Co/Mo = 1/3. These observations can be explained as follows. Decomposition of C_2H_5OH into CH_4, CO, C_2H_2, C_2H_4, H_2, H_2O, etc. in the gas phase is promoted at higher temperature and/or longer residence time in the reactor, and some of those decomposition products become precursors for CNTs in the area where Co/Mo = 1/3. Based on our simulations of the decomposition of C_2H_5OH by CHEMKIN with 57 chemical species and 372 elemental reactions [20, 21], Fig. 5 shows the time dependence of mole fractions at 4.0 kPa and 1120 K. In our experiments, decomposition products such as CO were generated, and enhanced growth of CNTs occurred at the Co/Mo ratio of 1/3, which is reportedly optimum for CO feedstock [4, 5, 11]. Further investigation is needed to clarify the mechanism of high catalytic activity with decomposition products in this area
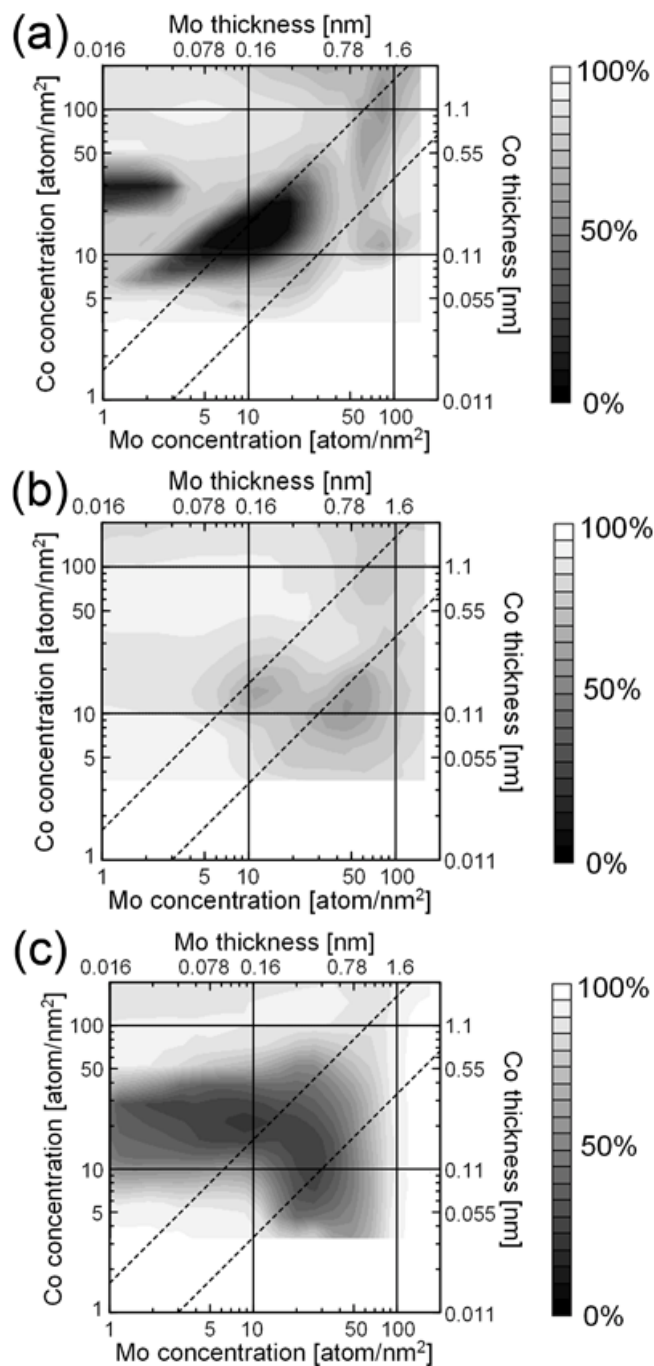
where Co/Mo = 1/3.

Fig. 4.   Maps of optical transmittance of catalyst library as a function of surface atomic concentrations of Co and Mo on quartz glass substrates after ACCVD. Temperature was 1120 K (a, c) and 1220 K (b), C_2H_5OH pressure was 4.0 kPa for all samples, and

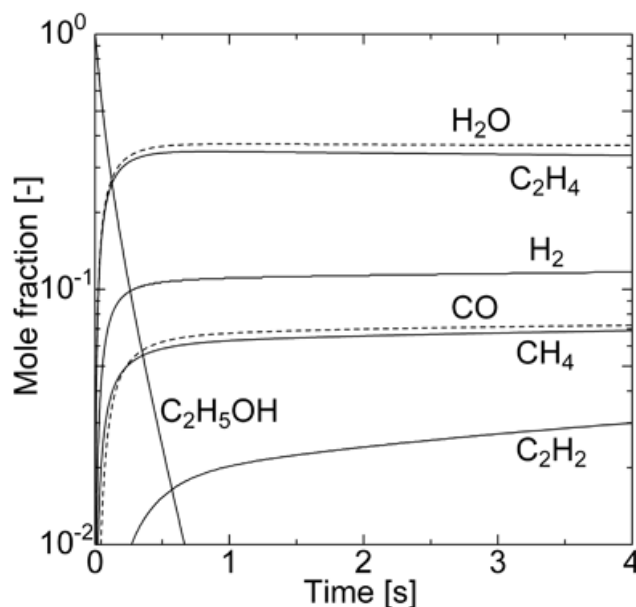C_2H_5OH flow rate was 25 sccm (a), 23 sccm (b), and 8.5 sccm (c).

Fig. 5. Time dependence of mole fractions in the gas-phase simulated by CHEMKIN [20, 21] during thermal decomposition of 4.0 kPa C_2H_5OH at 1120 K.

3.2 *Characterization of CNTs and catalyst nanoparticles*

Figure 6 shows cross-sectional SEM images and Fig. 7 shows TEM images and histograms of the CNT diameter distributions of as-grown CNTs obtained by using catalysts uniformly prepared on different substrates. In both figures, images (a)-(e) correspond to the locations indicated in Photographs I and II in Fig. 6, where the nominal thickness of Co/Mo (nm) was 0.11/0.28 (a), 0.22/0.14 (b, d), 0.070/0.047 (c), and 0.78/0 (e). Based on TEM observation, although some double-walled CNTs were evident, mainly single-walled CNTs were grown under these five conditions (a-e). Vertically aligned SWCNT forests were formed under two different catalyst conditions (b and e) and their maximum height was about 30 μm either at 1120 K (b) or 1020 K (e).

Therefore, these two catalyst conditions are optimum conditions. In this study, the optimum amounts of Co and Mo were smaller than those reported in our previous study [16]. The reason for this difference is that in our current study, we reduced the effect of carbon contamination from the physical mask used in the CMD method. Although the Co/Mo atomic ratio for condition (b) (Co/Mo = 2.2/1.0) is similar to that previously reported (Co/Mo = 1.6/1.0) [6, 7], condition (e) (Co without Mo) was identified in the present work as a condition that yields high catalytic activity. Note that this condition for high catalytic activity, on which vertically aligned SWCNT forest grew, contained only Co.

CNTs had average diameters of 2.7 nm (a), 2.6 nm (b, d) and 2.5 nm (c) and bimodal diameter distribution of 1-2 and 3-4 nm (2.5 nm average) (e) (Co without Mo). As seen in the insets of Fig. 6, the density of CNTs did not strongly depend on the Co/Mo ratio or on the CVD conditions. The diameter distribution of CNTs was unimodal for (a), somewhat irregularly shaped for (b, d), slightly bimodal for (c), and bimodal for (e). Interestingly, this order coincides with the order of Mo thickness, namely, 0.28 nm for (a), 0.14 nm for (b, d), 0.047 nm for (c), and 0 nm for (e). This correspondence suggests that Mo suppressed the surface diffusion of Co adatoms over SiO_2, and that in the Co catalysts without sufficient Mo content, Ostwald ripening occurred and resulted in the formation of Co particles with a bimodal diameter distribution.

Figure 8 shows the Raman spectra of samples (b) and (e) in Fig. 6 taken from the side of SWCNT forests at positions every 5 μm from the top to bottom by using a laser with three different wavelengths. RBM peaks weakened as the distance from the top increased, suggesting that the structure of the CNTs changed during growth. Note

that these data were obtained for substrates with uniform catalyst thickness, and therefore might apply to various VA-SWCNT growth methods that use catalysts supported on substrates. In the spectrum for sample (b) obtained using 633-nm-excitation, RBM peaks were clearly evident around 115 and 140 cm^{-1}, which correspond to CNT diameters of 2.2 and 1.8 nm, respectively. RBMs for lower wavenumbers, i.e., larger diameters, were rarely observed due to their smaller sensitivity and to signal suppression by optical filter cutting Rayleigh scattering. Note that these RBM peaks were not observed for sample (e). This result is consistent with the TEM results shown in Fig. 7e; SWCNTs had bimodal diameter distribution and their diameter tended to be either smaller than 2 nm or larger than 3 nm.
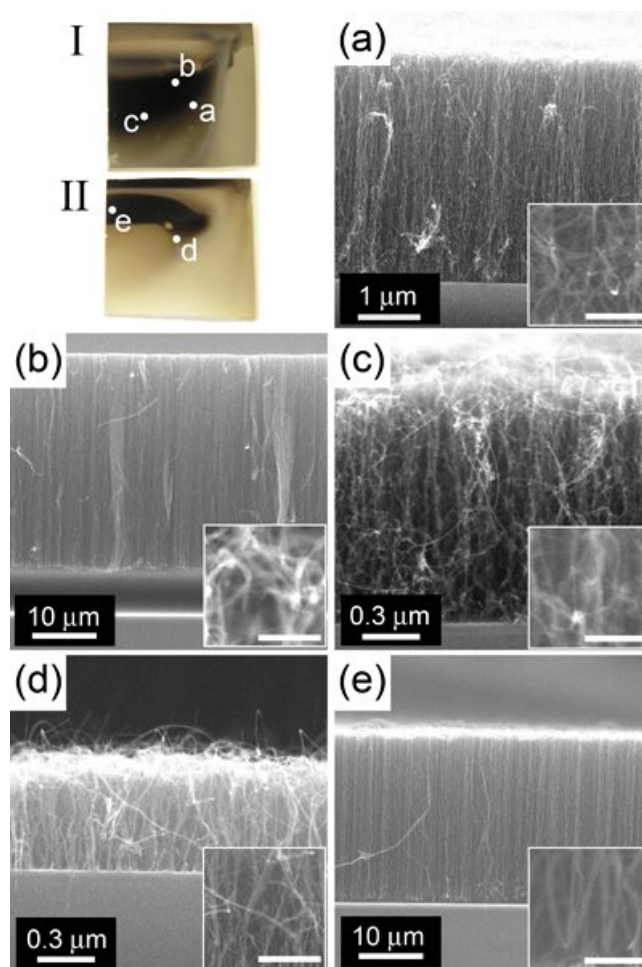
Fig. 6. Cross-sectional SEM images of samples with catalyst conditions at marked positions in photographs I and II, which are the same as the samples in Fig. 2 grown from 4.0 kPa C_2H_5OH at 1120 K (I) and 1020 K (II). Nominal thickness of Co/Mo (nm) was 0.11/0.28 (a), 0.22/0.14 (b, d), 0.070/0.047 (c), and 0.78/0 (e). Scale bar in insets is 100 nm.
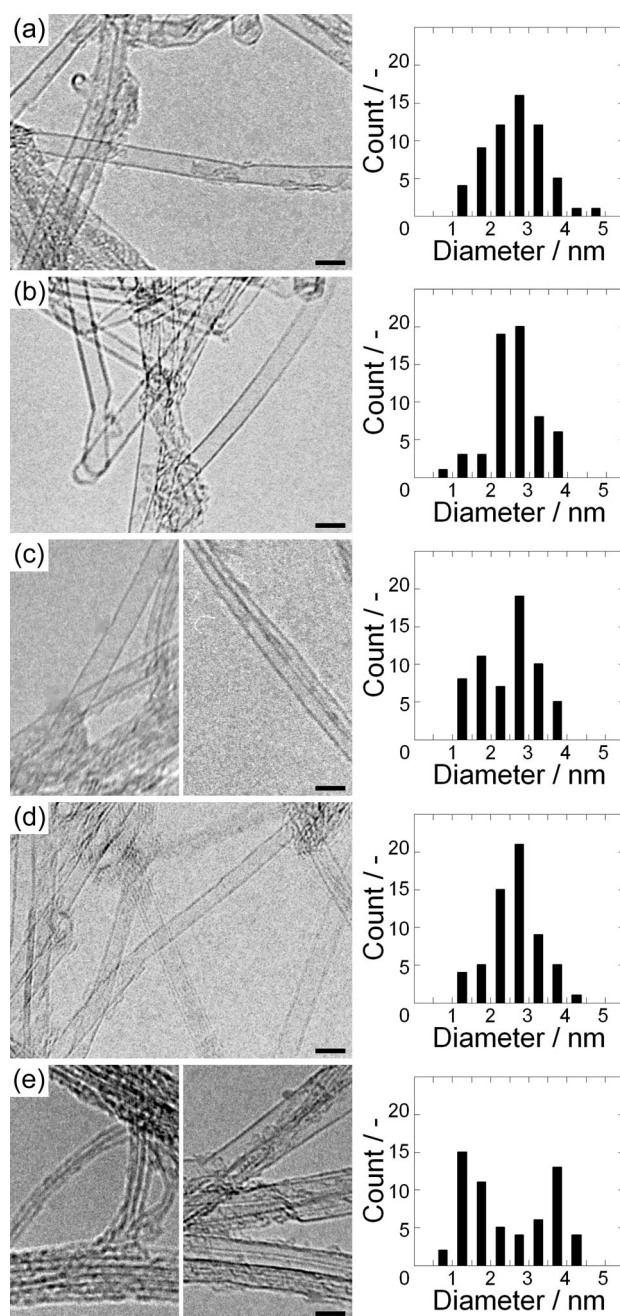
Fig. 7. TEM images and histograms of diameter distributions of SWCNTs in Figs. 6a-e. Scale bar in TEM images is 5 nm.
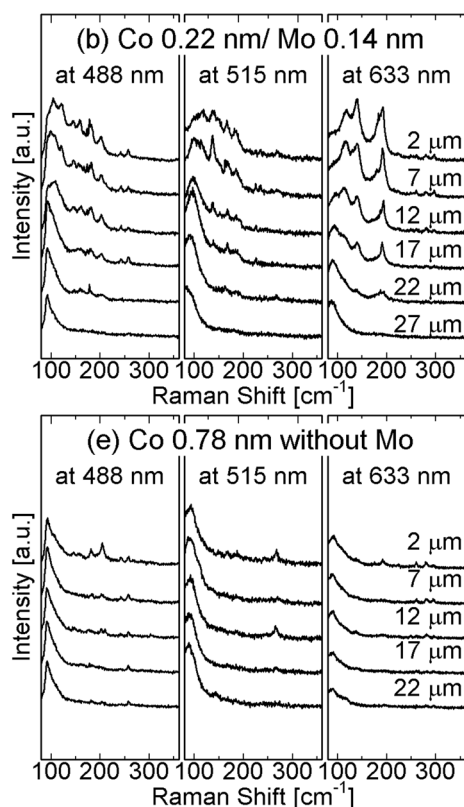
Fig. 8. Raman spectra for RBM regions of samples (b) and (e) in Fig. 6 taken from the side of SWCNT forests at positions every 5 μm from the top to bottom by using an excitation laser with three different wavelengths.

To investigate the reason for the structure changes in SWCNTs during CVD growth, catalyst nanoparticles were observed by using SEM. Figure 9 shows SEM images of a 0.78-nm-thick Co layer deposited on a Si substrate that had a 50-nm-thick thermal oxide layer. Although the particle structure could not be clearly observed in an as-deposited layer (Fig. 9a), particles were clearly evident after pretreatment under H_2 atmosphere at high temperature (Figs. 9b, d, f). Although the Co particles at 1020 K (Fig. 9b) and at 1120 K (Fig. 9d) showed similar structure, the structure significantly differed from that at 1220 K (Fig. 9f). This difference in structure at the higher reaction temperature might be due to Co reacting with SiO_2 and/or melting because the melting

point is lower for several-nanometer-sized particles than for bulk.

Figure 10 shows a photograph of a Co-Mo catalyst library after pretreatment under H_2 atmosphere at 1120 K followed by ACCVD at 1020 K with a C_2H_5OH pressure of 4.0 kPa. Comparing this figure with Fig. 2c, the shape of the black area is closer to that at 1020 K rather than that of 1120 K. The temperatures during CVD might affect the particle structure because metal particles form a solid solution with carbon during CNT growth, and solid solutions have a lower melting point than does a pure metal. In fact, in the present work, Co particles after CVD (Figs. 9c, 9e, 9g) had a coarser structure compared with as-reduced particles (Figs. 9b, 9d, 9f). Although the catalyst and CVD conditions (Co/Mo = 0.78/0nm, 4.0 kPa C_2H_5OH at 1020 K, respectively) for the SEM images in Figs. 9b (before CVD) and 9c (after CVD) are the same as those for the TEM images in Fig. 7e, we could not confirm the bimodal distribution of particle diameters due to the resolution limit of the SEM.
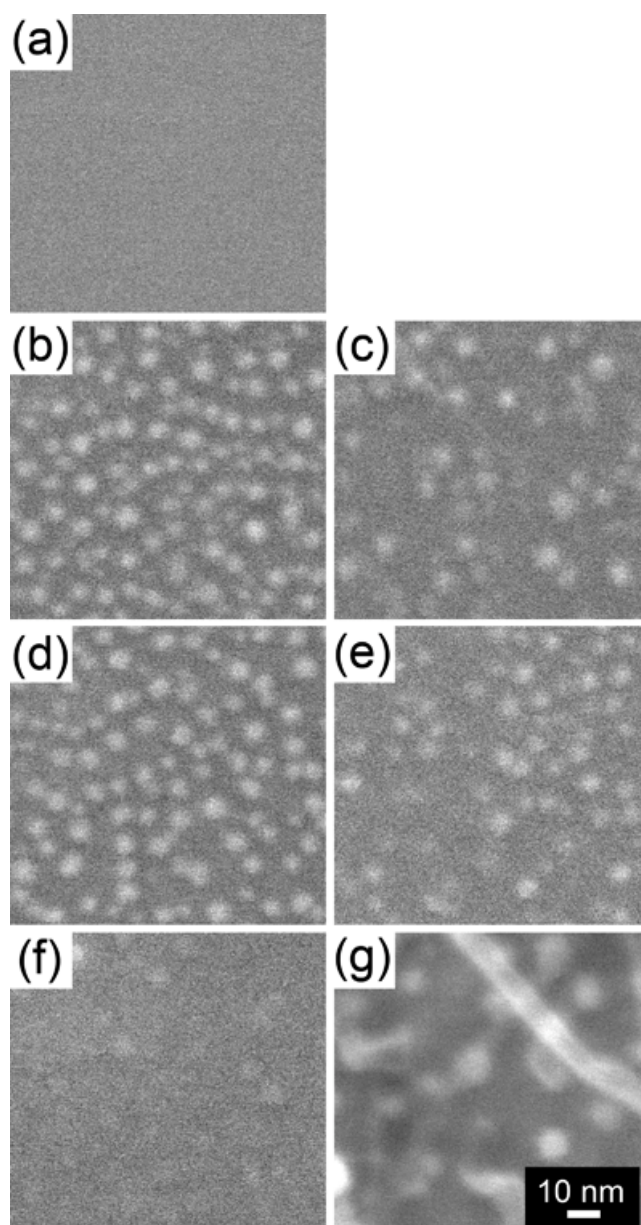
Fig. 9.　SEM images of a 0.78-nm-thick Co layer on SiO_2; as-deposited (a) and after pretreatment under H_2 atmosphere (b, d, f) and ACCVD at 1020 K (c, e, g). Temperature during pretreatment was 1020 K (b, c), 1120 K (d, e) and 1220 K (f, g). In (c) and (e), vertically aligned CNTs were removed with tweezers before observation to clearly view the surface, whereas in image (g), CNTs did not need to be removed because few CNTs grew.
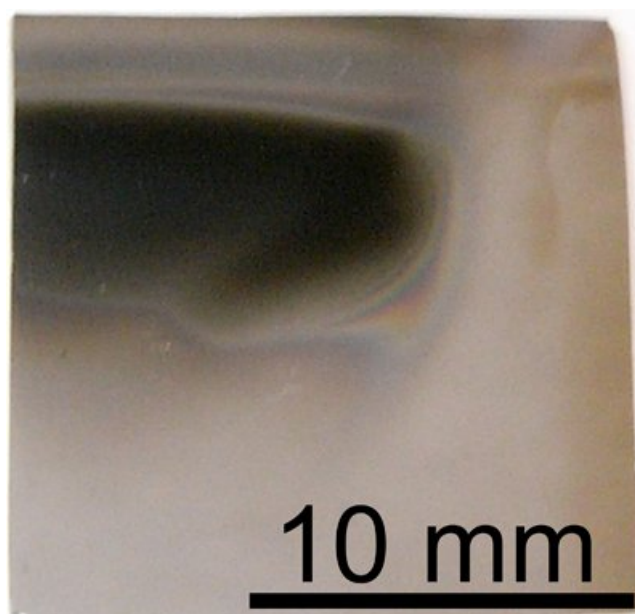
Fig. 10. Photograph of a Co-Mo catalyst library after pretreatment under H_2 atmosphere at 1120 K followed by ACCVD at 1020 K with 4.0 kPa C_2H_5OH.

3.3 *Growth mechanisms*

Our results revealed multiple optimum conditions for the growth of CNTs from C_2H_5OH with Co-Mo binary catalyst. These conditions depended on the CVD conditions, such as reaction temperature, C_2H_5OH pressure, and C_2H_5OH flow rate. The multiple optimum conditions can be understood in the context of CNTs growing from different carbon precursors and the precursor concentration depending on the CVD conditions.

At a reaction temperature of 1120 K and C_2H_5OH pressure of 4.0 kPa (center image in Fig. 2c, and Fig. 4a), the optimum thickness of Co for each Mo thickness was positively correlated with Mo thickness, although the relationship was not always linear. When the CVD conditions changed, other areas showed high catalytic activity (Figs. 2c, 4b and 4c). In conclusion, based on the result showing that the CNT growth areas were

18

bounded within a certain range, both the composition and amount of catalyst are important parameters. Therefore, stoichiometry can not completely explain the observations reported here.

Mo prevents the surface diffusion of Co, thus keeping the diameter of Co particles small while increasing the number density. When the amount of Mo decreased (Fig. 7c) or Co was used without Mo (Fig. 7e), SWCNTs with bimodal diameter distributions were obtained. This bimodal distribution of SWCNT diameters most likely was due to Ostwald ripening, resulting in the formation of a bimodal diameter distribution of Co particles. A number of methods have been proposed to prevent the aggregation of Co [4, 5, 7]. Based on our results, Mo as thin as a monolayer or thinner efficiently suppressed the broadening of CNT diameter distribution.

The catalyst nanoparticle diameter apparently governed the diameter of the individual nanotubes and the height of SWCNT forest depended strongly on the catalyst conditions. If SWCNTs have the same length and film density and if the number density of active catalyst nanoparticles is low, then we expect the SWCNTs to exhibit greater curvature as shown in Fig. 11b, however we could not confirm this from the insets of Fig. 6. Too much Mo inhibited the growth of SWCNTs (Figs. 6a and 6b), and the height of the SWCNT forest depended on the amounts of Co and Mo even when the Co/Mo atomic ratio was the same (Figs. 6b and 6c). More study is needed to understand the factors and conditions that determine the height of SWCNT forests.
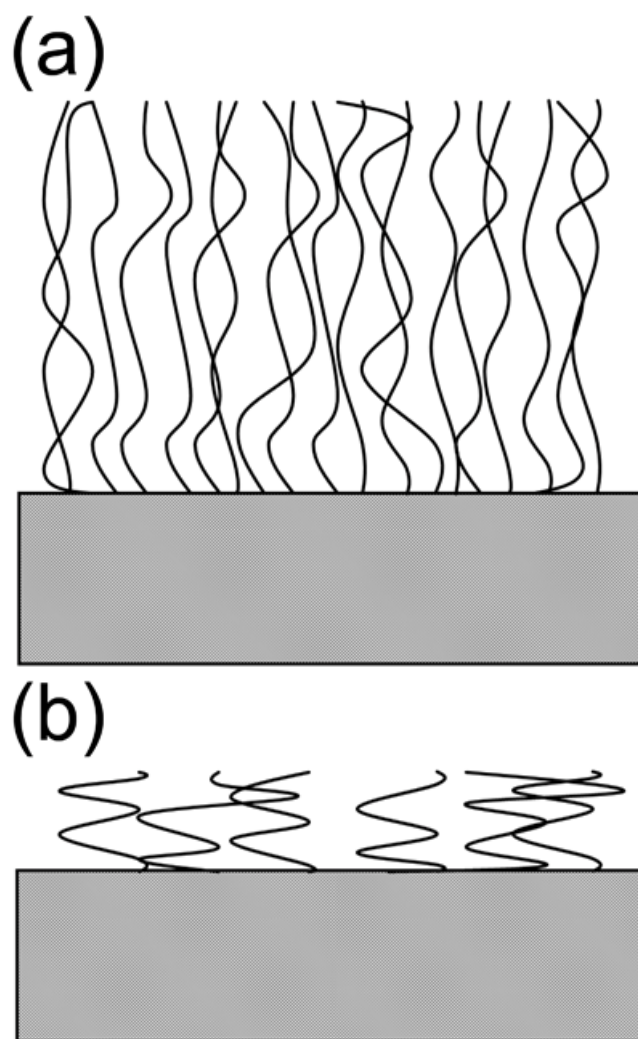
Fig. 11. Schematic of SWCNT forests at high (a) and low (b) number density

4. Conclusions

Using binary Co-Mo combinatorial catalyst library, we systematically investigated the relationship between catalyst and CVD conditions for CNT growth by ACCVD. Multiple high catalytic activity areas were identified, and found dependent on the ACCVD conditions and the different gas phase precursors. When a Co-Mo binary catalyst was used, vertically aligned SWCNT forests with an average diameter of 2-3 nm grew. Mo as thin as a monolayer or thinner suppressed the broadening of the

SWCNT diameter distribution, and both the composition and amount of Co and Mo affected the catalytic activity. A highly active catalytic condition using a Co catalyst was identified at a reaction temperature of 1020 K, and a vertically aligned SWCNT forest with a bimodal diameter distribution (1-2 nm and 3-4 nm) grew under this condition.

References

[1]   Colomer JF, Stephan C, Lefrant S, Van Tendeloo G, Willems I, Konya Z, et al. Large-scale synthesis of single-wall carbon nanotubes by catalytic chemical vapor deposition (CCVD) method. Chemical Physics Letters. 2000 Jan;317(1-2):83-9.

[2]   Colomer JF, Benoit JM, Stephan C, Lefrant S, Van Tendeloo G, Nagy JB. Characterization of single-wall carbon nanotubes produced by CCVD method. Chemical Physics Letters. 2001 Sep;345(1-2):11-7.

[3]   Tang S, Zhong Z, Xiong Z, Sun L, Liu L, Lin J, et al. Controlled growth of single-walled carbon nanotubes by catalytic decomposition of CH4 over Mo/Co/MgO catalysts. Chemical Physics Letters. 2001 Dec;350(1-2):19-26.

[4]   Herrera JE, Balzano L, Borgna A, Alvarez WE, Resasco DE. Relationship between the structure/composition of Co-Mo catalysts and their ability to produce single-walled carbon nanotubes by CO disproportionation. Journal of Catalysis. 2001 Nov;204(1):129-45.

[5]   Herrera JE, Resasco DE. Loss of single-walled carbon nanotubes selectivity by disruption of the Co-Mo interaction in the catalyst. Journal of Catalysis. 2004 Jan;221(2):354-64.

[6]   Murakami Y, Chiashi S, Miyauchi Y, Hu MH, Ogura M, Okubo T, et al. Growth of vertically aligned single-walled carbon nanotube films on quartz substrates and their optical anisotropy. Chemical Physics Letters. 2004 Feb;385(3-4):298-303.

[7]   Hu MH, Murakami Y, Ogura M, Maruyama S, Okubo T. Morphology and chemical state of Co-Mo catalysts for growth of single-walled carbon nanotubes vertically aligned on quartz substrates. Journal of Catalysis. 2004 Jul;225(1):230-9.

[8]   Hata K, Futaba DN, Mizuno K, Namai T, Yumura M, Iijima S. Water-assisted highly efficient synthesis of impurity-free single-waited carbon nanotubes. Science. 2004 Nov;306(5700):1362-4.

[9]   Zhong GF, Iwasaki T, Honda K, Furukawa Y, Ohdomari I, Kawarada H. Low temperature synthesis of extremely dense, and vertically aligned single-walled carbon nanotubes. Japanese Journal of Applied Physics Part 1-Regular Papers Short Notes & Review Papers. 2005 Apr;44(4A):1558-61.

[10]   Zhang GY, Mann D, Zhang L, Javey A, Li YM, Yenilmez E, et al. Ultra-high-yield growth of vertical single-walled carbon nanotubes: Hidden

roles of hydrogen and oxygen. Proceedings of the National Academy of Sciences of the United States of America. 2005 Nov;102(45):16141-5.

[11]   Zhang L, Tan YQ, Resasco DE. Controlling the growth of vertically oriented single-walled carbon nanotubes by varying the density of Co-Mo catalyst particles. Chemical Physics Letters. 2006 Apr;422(1-3):198-203.

[12]   Wang WH, Hong TH, Kuo CT. Super growth of vertically aligned SWCNTs using self-assembled nanoparticles from CoCrPtOx ultra-thin film. Carbon. 2007 Jan;45(1):97-102.

[13]   Nozaki T, Ohnishi K, Okazaki K, Kortshagen U. Fabrication of vertically aligned single-walled carbon nanotubes in atmospheric pressure non-thermal plasma CVD. Carbon. 2007 Feb;45(2):364-74.

[14]   Christen HM, Puretzky AA, Cui H, Belay K, Fleming PH, Geohegan DB, et al. Rapid growth of long, vertically aligned carbon nanotubes through efficient catalyst optimization using metal film gradients. Nano Letters. 2004 Oct;4(10):1939-42.

[15]   Saito T, Xu WC, Ohshima S, Ago H, Yumura M, Iijima S. Supramolecular catalysts for the gas-phase synthesis of single-walled carbon nanotubes. Journal of Physical Chemistry B. 2006 Mar;110(12):5849-53.

[16]   Noda S, Sugime H, Osawa T, Tsuji Y, Chiashi S, Murakami Y, et al. A simple combinatorial method to discover Co-Mo binary catalysts that grow vertically aligned single-walled carbon nanotubes. Carbon. 2006 Jul;44(8):1414-9.

[17]   Noda S, Tsuji Y, Murakami Y, Maruyama S. Combinatorial method to prepare metal nanoparticles that catalyze the growth of single-walled carbon nanotubes. Applied Physics Letters. 2005 Apr;86(17).

[18] Maruyama S, Kojima R, Miyauchi Y, Chiashi S, Kohno M. Low-temperature synthesis of high-purity single-walled carbon nanotubes from alcohol. Chemical Physics Letters. 2002 Jul;360(3-4):229-34.

[19] Murakami Y, Chiashi S, Miyauchi Y, Maruyama S. Direct synthesis of single-walled carbon nanotubes on silicon and quartz-based systems. Japanese Journal of Applied Physics Part 1-Regular Papers Short Notes & Review Papers. 2004 Mar;43(3):1221-6.

[20] Kee RJ, Rupley FM, Miller JA. Chemkin-II: A Fortran Chemical Kinetics Package for the Analysis of Gas-Phase Chemical Kinetics. Sandia Report. 1995;SAND89:8009B.

[21] Marinov NM. A detailed chemical kinetic model for high temperature ethanol oxidation. International Journal of Chemical Kinetics. 1999 Mar;31(3):183-220.

Figure captions

Fig. 1. Top-view schematic of novel ACCVD apparatus

Fig. 2. Schematic of a Co-Mo catalyst library (a), nominal thickness profiles of Co and Mo within the catalyst library (b), and photographs of libraries after ACCVD at different reaction temperature and C_2H_5OH pressure (c).

Fig. 3. Photograph and Raman spectra of a Co-Mo catalyst library after ACCVD at reaction temperature of 1120 K and C_2H_5OH pressure of 4.0 kPa (same sample as that in the center image of Fig. 2c). White dots indicate locations at which Raman spectra were obtained using an Ar^+-laser (488.0 nm) for excitation.

Fig. 4. Maps of optical transmittance of catalyst libraries as a function of surface atomic concentrations of Co and Mo on quartz glass substrates after ACCVD.

Temperature was 1120 K (a, c) and 1220 K (b), C_2H_5OH pressure was 4.0 kPa for all samples, and C_2H_5OH flow rate was 25 sccm (a), 23 sccm (b), and 8.5 sccm (c).

Fig. 5. Time dependence of mole fractions in the gas-phase simulated by CHEMKIN [20, 21] during thermal decomposition of 4.0 kPa C_2H_5OH at 1120 K.

Fig. 6. Cross-sectional SEM images of samples with catalyst conditions at marked positions in photographs I and II, which are the same as the samples in Fig. 2 grown from 4.0 kPa C_2H_5OH at 1120 K (I) and 1020 K (II). Nominal thickness of Co/Mo (nm) was 0.11/0.28 (a), 0.22/0.14 (b, d), 0.070/0.047 (c), and 0.78/0 (e). Scale bar in insets is 100 nm.

Fig. 7. TEM images and histograms of diameter distributions of SWCNTs in Figs. 6a-e. Scale bar in TEM images is 5 nm.

Fig. 8. Raman spectra for RBM regions of samples (b) and (e) in Fig. 6 taken from the side of SWCNT forests at positions every 5 μm from the top to bottom by using an excitation laser with three different wavelengths.

Fig. 9. SEM images of a 0.78-nm-thick Co layer on SiO_2; as-deposited (a) and after pretreatment under H_2 atmosphere (b, d, f) and ACCVD at 1020 K (c, e, g). Temperature during pretreatment was 1020 K (b, c), 1120 K (d, e) and 1220 K (f, g). In (c) and (e), vertically aligned CNTs were removed with tweezers before observation to clearly view the surface, whereas in image (g), CNTs did not need to be removed because few CNTs grew.

Fig. 10. Photograph of Co-Mo catalyst library after pretreatment under H_2 atmosphere at 1120 K followed by ACCVD at 1020 K with 4.0 kPa C_2H_5OH.

Fig. 11. Schematic of SWCNT forests at high (a) and low (b) number density